

А. М. Халил*, И. С. Логинова, В. С. Золоторевский

National University of Science and Technology, Moscow

**eng.asmaa.m.khlil@outlook.com*

Supervisor – Prof., V. S. Zolotorevsky

**ИССЛЕДОВАНИЕ ВЛИЯНИЯ ПАРАМЕТРОВ ЛАЗЕРНОЙ СВАРКИ НА
МИКРОСТРУКТУРУ И МЕХАНИЧЕСКИЕ СВОЙСТВА
Al–4,7 % Mg–0,32 % Mn–0,21 % Sc–0,09 % Zr СПЛАВА**

В работе исследовано влияние пиковой мощности (0,64–1,31 кВт) при напряжениях из диапазона 330–430 В при лазерной сварке со стандартным диаметром пучка и длительностью импульса 8 мс. Изучена микроструктура, сформированная сваркой. Установлено, что существует разнообразие в размерах и форме зерен в зоне шва. Показано, что с увеличением пиковой мощности ширина и глубина области шва увеличивается.

Ключевые слова: деформируемые алюминиевые сплавы, лазерная сварка, пиковая мощность, микроструктура.

A. M. Khalil, I. S. Loginova, V. S. Zolotorevsky

**INVESTIGATION OF INFLUENCE OF PARAMETERS OF LASER
WELDING ON MICROSTRUCTURE AND MECHANICAL PROPERTIES
OF Al–4.7 % Mg–0.32 % Mn–0.21 % Sc–0.09 % Zr ALLOY**

In the present work the influence of peak power of laser beam welding were studied at voltage range from 330 to 430 V and peak power (0,64; 0,75; 0,87; 1,01; 1,15; 1,31) kW, and laser beam diameter is standard and duration 8 ms. The microstructure after welding was studied. It was concluded that there is a variant in grain size and shape in the welded zone and pre-welded area. The dimensions of welded zone was measured. From measuring data, it was observed, that as increasing the peak power the width and depth of welding increased.

Keyword: deformed aluminum alloy, laser welding, peak power, microstructure.

Al–Mg alloys have been widely used in the field of food handling and chemical processing industries because of their attractive comprehensive properties such as medium strength, high ductility and excellent corrosion resistance [1–4]. The strength of these alloys is primarily due to solid solution strengthening by Mg, which has a substantial solid solubility in aluminum. However, in order to broaden the application in automotive and aerospace

industries, alloys with higher mechanical strength are required. An effective approach to improve the strength of aluminum alloys, including our experimental Al–Mg alloys, is the addition of scandium as an alloying element [5–6]. The strengthening mechanism of Al-alloys with Sc addition has been frequently reported to be the presence of Nano-scaled coherent Al₃Sc particles that precipitated from supersaturated α -Al matrix during aging treatment or thermo-mechanical processing [7–12]. For the cast ingots, on the other hand, the formation of primary Al₃Sc particles also helps refine the microstructure, which improves both the strength and formability. However, such effect shows up only when Sc addition reaches eutectic composition [13–15]. Owing the great contribution of grain refinement, much of the work on the Al₃Sc primary particles found in aluminum alloys containing a high level of scandium have been carried out in numerous studies [16–17].

The material used in the present work was 1545 K alloy with the chemical composition presented in Table 1. This alloy from a 280-mm-thick industrial ingot, sheets with thicknesses of 10 mm. The 10-mm sheets were rolled to a thickness of 1 mm using a laboratory rolling mill. Heat treatment was performed using a “Nabertherm” furnace with a temperature accuracy of ± 1 °C.

We used technology involved only cold (at room temperature) rolling with one intermediate annealing step at 250 °C for 1 h , and then prepared it by Struers (grinding and polishing equipment) and then did oxidation process to obtain good photos of microstructure by microscope Neophot-30.

Table 1

Chemical composition of the investigated alloy 1545 K, mas. %

Al	Mg	Mn	Sc	Zr	Be	Cu	Fe	Zn
bal.	4.7	0.32	0.21	0.09	0.001	<0.1	<0.1	<0.1

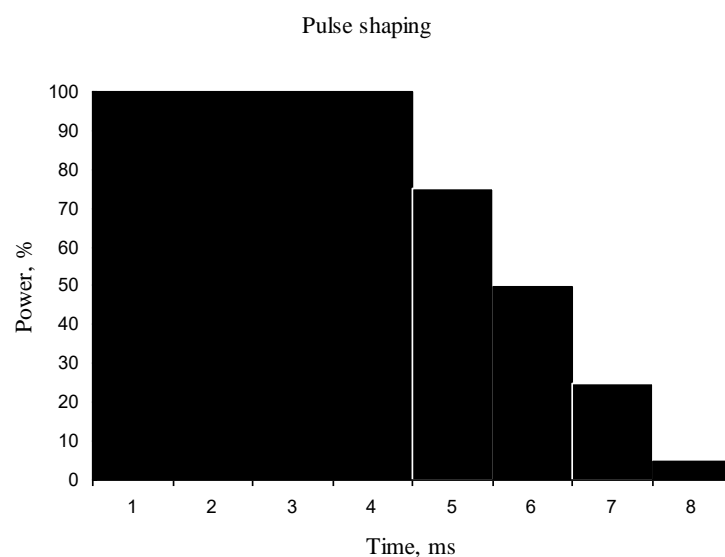


Figure 1. The form of pulse shape

Table2 shows the results of width and depth after welding with different voltages (330, 350, 370, 390, 410, 430 volt) and the beam diameter is standard. Print tracks at a constant pulse duration of 8 ms, a constant rate of movement of table 1 mm/sec, a constant overlap of 0,1 mm, and the pulse shape in the next figure.

Table 2

Results of width and depth after welding with a parameters peak power and voltage

No. track	Voltage, V	Peak power, kW	Depth, mm	Width, mm
1	330	0,64	55,0	386,6
2	350	0,75	71,5	401,9
3	370	0,87	105,9	491,0
4	390	1,01	132,1	626,3
5	410	1,15	182,3	701,2
6	430	1,31	235,7	730,0

After laser welding a samples were prepared and obtained the microstructure of welded zone by oxidation process. The photos are presented at figure 2.

From the previous figure 2, we can observed that after cold rolling the material have elongated grains due to plastic deformation and after laser welding this grains transformed to various shape of grains like small equiaxed ‘chill crystals’, columnar and large equiaxed grains due to the direction of heat.

Small **equiaxed grains (chill crystals)** form at this stage. Latent crystallization heat, liberating from the crystallizing metal, decreases the undercooling of the melt and depresses the fast grains growth. At this stage some of small grains, having favorable growth axis, start to grow in the direction opposite to the direction of heat flow. As a result **columnar crystals (columnar grains)** form. Length of the columnar grains zone is determined by the **constitutional undercooling**. When the temperature of the fusion weld, adjacent to the solidification front, increases due to the liberation of the latent heat, constitutional undercooling will end and the columnar grains growth will stop. Further cooling of the molten alloy in the central zone of the ingot will cause formation of **large equiaxed grains**.

Finally, from the figure 3 as seen as peak power increases the depth and width of welded zone increased.

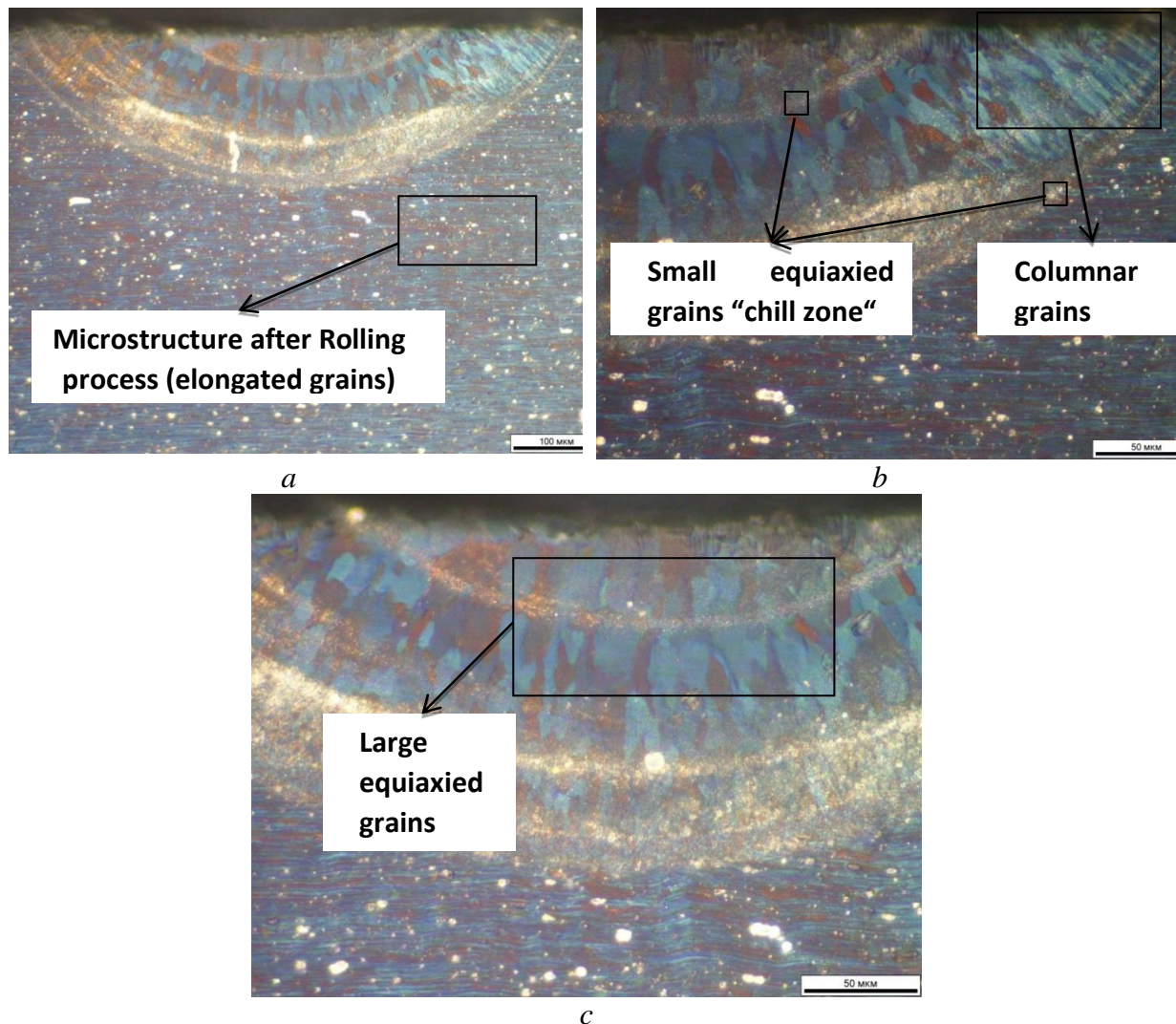


Figure 2. Some microstructures of 1545 K alloy after laser welding with parameter peak power (a, b and c)

Conclusion

1. The material used in the present work was 1545 K alloy, we make laser welding process with voltage from 330 to 430 Volt, and different peak power (0,64; 0,75; 0,87; 1,01; 1,15; 1,31) kW, and laser beam diameter is standard and duration 8 ms.

2. Obtained microstructure photos are shown the welded area and measured the dimension of welded area to choose the suitable voltage and peak power to weld this material, and get the shape of grains after welding and discuss it. And, it was observed, that as increasing the peak power the width and depth of welding increased.

The work was performed as part of the state work "Carrying out of research work (basic research, applied research and experimental development)" state task MES of Russia in the sphere of scientific activities 2014–2016. (Task № 2014/113).

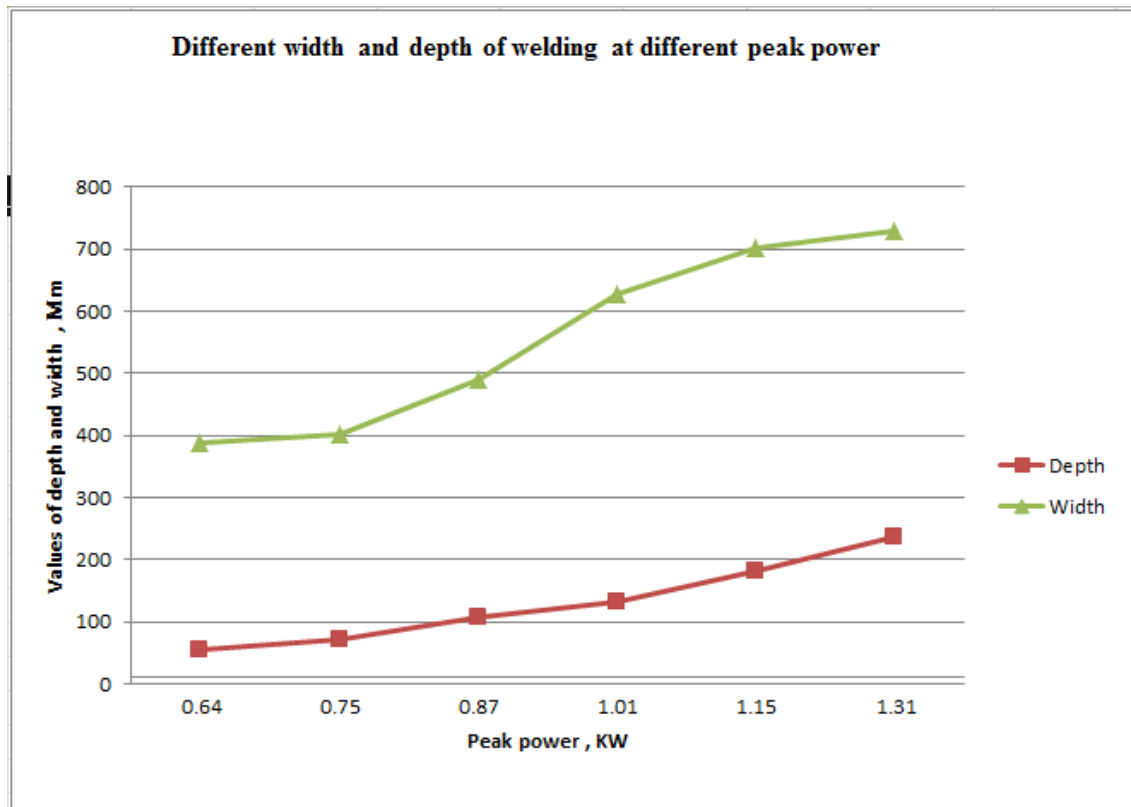


Figure 3. Different width and depth of welding at different peak power

Referances

1. The effect of erbium on the microstructure and mechanical properties of Al–Mg–Mn–Zr alloy / S. P. Wen [et al.] // Mater. Sci. Eng. A 516 (2009) P. 42–49.
2. Microstructure dependent fatigue crack growth in Al–Mg–Sc alloy / M. J. Li [et al.] // Mater. Sci. Eng. A 611 (2014) P. 142–151.
3. Influence of annealing temperature on the baking response and corrosion properties of an Al–4.6 wt% Mg alloy with 0.54 wt% Cu / A. Alil [et al.] // J. Alloys Compd. 625 (2015) P. 76–84.
4. Lathabai S., Lloyd P. G. The effect of scandium on the microstructure, mechanical properties and weldability of a cast Al–Mg alloy // Acta Mater. 50 (2002) 4275–4292.
5. The effect of Sc additions on the microstructure and age hardening behaviour of as cast Al–Sc alloys / S. Costa [et al.] // Mater. Des. 42 (2012) P. 347–352.
6. New Al–Mg–Sc alloys / Y.A. Filatov [et al.] // Mater. Sci. Eng. A 280 (2000) P. 97–101.
7. Characterization of a laserfabricated hypereutectic Al–Sc alloy bar / P. A. Rometsch [et al.] // Scr. Mater. 87 (2014) P. 13–16;
8. Influence of welding parameter on mechanical properties and fracture behavior of friction stir welded Al–Mg–Sc joints / Y. Tao [et al.] // Mater. Sci. Eng. A 612 (2014) P. 236–245.

9. Characteristics of aluminium–scandium alloy thin sheets obtained by physical vapour deposition/ H. R. Stock [et al.] // Mater. Des. 31 (2010) P. 576–581.
10. Apps P. J., Berta M., Prangnell P. B. The effect of dispersoids on the grain refinement mechanisms during deformation of aluminium alloys to ultra-high strains // Acta Mater. 53 (2005) P. 499–511.
11. Jones M. J., Humphreys F.J. Interaction of recrystallization and precipitation: the effect of Al₃Sc on the recrystallization behaviour of deformed aluminium // Acta Mater. 51 (2003) P. 2149–2159.
12. Novotny G. M., Ardell A. J. Precipitation of Al₃Sc in binary Al–Sc alloys // Mater. Sci. Eng. A 318 (2001) P. 144–154.
13. Dynamic response and microstructure control of Al–Sc binary alloy under high-speed impact / W. G. Zhang [et al.] // Mater. Sci. Eng. A 578 (2013) P. 35–45;
14. Scientific principles of making an alloying addition of scandium to aluminium alloys / V.G. Davydov [et al.] // Mater. Sci. Eng. A 280 (2000) P. 30–36.
15. Effect of scandium on the microstructure and ageing behaviour of cast Al–6Mg alloy / M. S. Kaiser [et al.] // Mater. Charact. 59 (2008) P. 1661–1666;
16. Norman A. F., Prangnell P. B., McEwen R. S. The solidification behaviour of dilute aluminium– scandium alloys // Acta Mater. 46 (1988) P. 5715–5732.
17. Hyde K. B., Norman A. F., Prangnell P. B. The effect of cooling rate on the morphology of primary Al₃Sc intermetallic particles in Al–Sc alloys // Acta Mater. 49 (2001) P. 1327–1337.